Scientific
Research
Publishing

Analysis and Design of 4 × 4 MIMO-Antenna Systems in Mobile Phone

Deshun Sun, Chongyu Wei

Qingdao University of Science & Technology, Qingdao, China
Email: 811093787@qq.com

Abstract

MIMO antenna systems can greatly improve the capacity and transmission rate of wireless communication. In this letter, two four-port multiple-input-multiple-output (MIMO) antenna systems are proposed in mobile devices. An algorithm of calculating envelope correlation (ρ_e) between antenna units is also proposed. By this algorithm the ρ_e of the PIFA-MIMO antenna system has been calculated. First, a PIFA-MIMO antenna system is designed for ISM (2.4 GHZ) application. The slots are etched on the ground and the antenna units are placed in such a way that the polarization diversity is exploited to enhance the impedance matching and isolation. Based on this, a printed wideband MIMO antenna system is proposed for portable 3G and 4G applications by means of multi-branch and the defect of ground technology, increasing the bandwidth and reducing mutual coupling between the antennas. The simulation results show that the return loss and isolation of the two antenna systems can meet the performance requirements of the antennas in the mobile phone.

1. Introduction

With the rapid development of wireless communication technology and the increasing demand of multimedia service, it is extremely urgent to realize the data communication with high speed and large capacity. As the core technology of wireless communication, MIMO technology has not only achieved a great increase in the capacity of communication, but also greatly improved the communication quality. By the literature [1], the capacity of the MIMO systems can be increased by the MIMO systems when channels are independent and identically dis-

tributed. The number and spacing of antennas are the key parameters of the MIMO antenna. Theoretically, the more the number of antennas are, the better the performance is. However, in the mobile phone and other small mobile terminals, with multiple antennas, antenna spacing between the antennas is not enough to ensure to reach high isolation between antennas. Actually, there are technical challenges in implementing mobile antennas with both a low correlation property and a sufficient antenna gain in mobile devices. If the isolation within the multi-antenna system is insufficient, system performance is reduced in terms of the gain and correlation due to the coupling between antennas [2].

In recent years, multiple-input-multiple-output (2 × 2 MIMO) communication systems use the multiple antennas that are equipped at receiver and transmitter ends to enhance not only the available data rate but the capacity in multipath environments. In order to improve the isolation between the two ports of the MIMO antenna, many designs have adopted the defect ground structure to meet the requirements of high isolation in MIMO antenna [3] [4]. [3] designs an ultra wideband (UWB) antenna. T he seam gap and vertical polarization are combined to improve the isolation between two antennas in band of 3 - 4.5 GHZ. [4] shows that the MIMO system is composed of two symmetrical printed monopole antenna. A high isolation between antenna elements can be obtained with two inverted L-branch and a rectangular slots embedded in the floor. The letter [5] investigates a method to use the DGS to the dual-band antenna with high port-isolation. Study [6] provides a design of two-port UWB MIMO antenna system with high isolation using a fork-shaped structure. An ultra wideband (UWB) MIMO antenna is designed in [7], which uses the floor gap and the vertical polarization mode to effectively improve the isolation of the two antennas in the 3 - 4.5 GHZ band. Antenna designs of 4 × 4 MIMO system have been realized in the literature [8] and [9]. [8] is a compact printed ultra wideband antenna and the antenna uses the EBG structure. In order to reduce the coupling between antenna elements, the four antenna elements are arranged vertically to achieve vertical polarization effect; in the design of [9], UWB antenna is a printed dipole antenna, and antenna element is also arranged vertically to achieve high isolation between the antennas. Based on these, in this paper, I design two new 4 × 4 MIMO antenna model. One works in a single frequency 2.4 GHZ (ISM), and the other can cover large bandwidth in 3G and 4G-LTE.

2. Correlation Analysis of MIMO Antennas Systems

2.1. Key Parameters of Diversity Antenna

Beyond the existing performance standards for a single-receiver mobile device, there are two antenna parameters that impact mobile receive diversity (MRD) performance: 1) the gain difference between the two antennas, and 2) the fading (envelope) correlation coefficient, ρ_e, between the two antennas.

2.2. Envelope Correlation Coefficient (ρ_e)

ρ_e is the most relevant to overall diversity performance. It is directly related to diversity gain (fading mitigation), and is statistically related to interference rejection gain.

2.2.1. Envelope Correlation Coefficient (ρ_e)

The fading (envelope) correlation coefficient ρ_e is a key indicator of MRD performance, and is strongly influenced by the incident EM field characteristics. The wireless multipath channel—due to its significant impact on the incident EM field must be considered as well as the antenna array and each element within the array.

Let me identify one of two mobile antenna ports. According to [10], the signal observed at each antenna port due to the kth multipath is a function of the antenna field pattern $E_m(\theta,\phi)$ and the incident field $F_m^k(\theta,\phi)$.

$$
\begin{aligned}
V_{Lm}^k &= \int_0^{2\pi}\int_0^{\pi} E_m(\theta,\phi)\cdot F_m^k(\theta,\phi)\cdot\sin\theta\cdot\mathrm{d}\theta\cdot\mathrm{d}\phi \\
&= \int_0^{2\pi}\int_0^{\pi}\left[E_{\theta,m}(\theta,\phi)\cdot F_{\theta,m}^k(\theta,\phi)+E_{\varphi,m}(\theta,\phi)\cdot F_{\varphi,m}^k(\theta,\phi)\right]\cdot\sin\theta\cdot\mathrm{d}\theta\cdot\mathrm{d}\phi
\end{aligned}
\tag{1}
$$

$E_{\theta,m}(\theta,\phi)$ and $E_{\varphi,m}(\theta,\phi)$ are the vertical and horizontal (respectively) polarization patterns of antenna m. It is assumed that the incident fields from different directions and polarizations are independent from one another.

The variance of the total received signal can be expressed as follows:

$$E\left[\left|V_{Lm}^{k}\right|^{2}\right]=P_{V}\int_{0}^{2\pi}\int_{0}^{\pi}\left|E_{\theta,m}\left(\theta,\phi\right)\right|^{2}\cdot P_{\theta}\left(\theta,\phi\right)\cdot\sin\theta\cdot\mathrm{d}\theta\cdot\mathrm{d}\phi+P_{H}\int_{0}^{2\pi}\int_{0}^{\pi}\left|E_{\phi,m}\left(\theta,\phi\right)\right|^{2}\cdot P_{\phi}\left(\theta,\phi\right)\cdot\sin\theta\cdot\mathrm{d}\theta\cdot\mathrm{d}\phi \quad (2)$$

$P_{\theta}\left(\theta,\phi\right)$ and $P_{\phi}\left(\theta,\phi\right)$ are the angular density functions of the vertically and horizontally polarized components of the incident field, both contributing to the total incident field. P_{V} and P_{H} are the mean powers that would be received by isotropic vertical and horizontal polarized antennas.

Similarly, the cross-correlation between the complex signal-envelopes received at the two antennas can be expressed as follows:

$$E\left[V_{L_{1}}^{k}\cdot V_{L_{2}}^{k\,*}\right]=E\left[V_{L_{\theta,1}}^{k}\cdot V_{L_{\theta,2}}^{k\,*}\right]+E\left[V_{L_{\varphi,1}}^{k}\cdot V_{L_{\varphi,2}}^{k\,*}\right]$$

$$=P_{H}\cdot\int_{0}^{2\pi}\int_{0}^{\pi}\left[XPR\cdot E_{\theta,1}\left(\theta,\varphi\right)\cdot E_{\theta,2}^{\,*}\left(\theta,\phi\right)\cdot P_{\theta}\left(\theta,\phi\right)+E_{\varphi,1}\left(\theta,\phi\right)\right. \quad (3)$$

$$\left.\cdot E_{\theta,2}^{\,*}\left(\theta,\phi\right)\cdot P_{\theta}\left(\theta,\phi\right)+E_{\varphi,1}\left(\theta,\phi\right)\cdot\sin\theta\cdot\mathrm{d}\theta\cdot\mathrm{d}\phi\right.$$

XPR is the cross-polarization power ratio, $XPR = P_{V}/P_{H}$. Using the two signal variances and the cross-correlation, the complex correlation coefficient can be calculated as follows:

$$\rho=\frac{E\left[V_{L1}^{k}\cdot V_{L2}^{k\,*}\right]}{\sqrt{E\left[V_{L1}^{k}\cdot V_{L1}^{k\,*}\right]\cdot E\left[V_{L2}^{k}\cdot V_{L2}^{k\,*}\right]}} \quad (4)$$

The envelope correlation ρ_{e} is defined as the correlation coefficient of the signal envelopes received at the two antenna ports. It is approximately equal to the magnitude-square of the complex correlation coefficient:

$$\rho_{e}\cong\left|\rho\right|^{2}=\frac{\left|E\left[V_{L1}^{k}\cdot V_{L2}^{k\,*}\right]\right|^{2}}{E\left[V_{L1}^{k}\cdot V_{L1}^{k\,*}\right]\cdot E\left[V_{L2}^{k}\cdot V_{L2}^{k\,*}\right]} \quad (5)$$

2.2.2. Incident Field Distribution Models

In order to compute the variance and correlation, the wireless channel is modeled to specify the incident field angular density function (or incident field distribution). The incident field distribution depends upon the scattering properties of the wireless environment. The most common assumption is that there are numerous scatterers present around the mobile, causing a uniform incident field in azimuth. Gaussian and Laplacian distributions are also used for cases when the incident wave is more concentrated from certain directions (smaller angular spread).

Several example incident field distribution expressions are provided below; they are all applicable to both polarizations and are all linear functions (not logarithmic).

1. Uniform in both azimuth and elevation:

$$P\left(\theta,\phi\right)=\frac{1}{4\pi}\quad 0<\theta<\pi\ \text{ and }\ 0<\phi<2\pi \quad (6)$$

2. Uniform in azimuth, Gaussian in elevation:

$$P\left(\theta,\phi\right)=A1\cdot\exp\left\{-\frac{\left[\theta-m_{\theta}\right]^{2}}{2\sigma_{\theta}^{2}}\right\}\quad 0<\theta<\pi\ \text{ and }\ 0<\phi<2\pi \quad (7)$$

3. Gaussian in both azimuth and elevation:

$$P\left(\theta,\phi\right)=A2\cdot\exp\left\{-\frac{\left[\phi-m_{\phi}\right]^{2}}{2\sigma_{\phi}^{2}}\right\}\cdot\exp\left\{-\frac{\left[\theta-m_{\theta}\right]^{2}}{2\sigma_{\theta}^{2}}\right\} \quad (8)$$

$$0<\theta<\pi\ \text{ and }\ 0<\phi<2\pi$$

m_{ϕ} and σ_{ϕ} are the mean and the standard deviation of the azimuth angle of arrivals. $A2$ is a scaling constant that forces the density function to unity when integrated over the surface of a unit sphere.

2.2.3. Calculating ρ_e at Discrete Angles

In engineering, the envelope correlation coefficient is calculated from the measured complex quantities $E_{\theta,1}(\theta,\phi)$, $E_{\phi,1}(\theta,\phi)$ and $E_{\theta,2}(\theta,\phi)$, $E_{\phi,2}(\theta,\phi)$. Recognizing that measurements occur at discrete angles, the expressions for ρ_e variables can be rewritten as follows:

$$R_{12} = \sum_{j=1}^{N\varnothing}\sum_{i=1}^{N\theta}\left(XPR\cdot E\theta1_{i,j}\cdot E\theta2_{i,j}^{*}\cdot P\theta_i + E\varnothing1_{i,j}\cdot E\varnothing2_{i,j}^{*}\cdot P\varnothing_j\right)\cdot\sin\theta_i\cdot\Delta\theta\cdot\Delta\varnothing$$

$$\sigma_1 = \sum_{j=1}^{N\varnothing}\sum_{i=1}^{N\theta}\left(XPR\cdot E\theta1_{i,j}\cdot E\theta1_{i,j}^{*}\cdot P\theta_i + E\varnothing1_{i,j}\cdot E\varnothing1_{i,j}^{*}\cdot P\varnothing_j\right)\cdot\sin\theta_i\cdot\Delta\theta\cdot\Delta\varnothing$$

$$\sigma_2 = \sum_{j=1}^{N\varnothing}\sum_{i=1}^{N\theta}\left(XPR\cdot E\theta2_{i,j}\cdot E\theta2_{i,j}^{*}\cdot P\theta_i + E\varnothing2_{i,j}\cdot E\varnothing2_{i,j}^{*}\cdot P\varnothing_j\right)\cdot\sin\theta_i\cdot\Delta\theta\cdot\Delta\varnothing$$

$XPR = P_V/P_H$; $p\theta$ and $p\phi$ are the incident field power densities defined in the previous section. $\Delta\theta$ and and $\Delta\phi$ are the angular increments for the measurement, and $N\theta$ and $N\phi$ are the number of angular measurement points in θ and ϕ assuming the measurement is done over a sphere of angles(θ varies from 0 to π and ϕ varies from 0 to 2π).

Finally, the envelope correlation coefficient is calculated from:

$$\rho_e = \frac{\left|R_{12}\right|^2}{\sigma_1\cdot\sigma_2} \tag{9}$$

2.2.4. Other ρ_e Techniques

The complex antenna pattern correlation method recommended above takes into account many factors that can impact the correlation between signals from dual antennas on handsets in a mobile environment. The designer may prefer to use more simple and rapid method to estimate the envelope correlation coefficient. For example, S Blanch *et al.* describes a calculation of envelope correlation coefficient using S formula:

$$\rho_e = \frac{\left|S_{11}*S_{12} + S_{21}*S_{22}\right|^2}{\left(1-\left(\left|S_{11}\right|^2+\left|S_{21}\right|^2\right)\right)\left(1-\left(\left|S_{21}\right|^2+\left|S_{12}\right|^2\right)\right)} \tag{10}$$

Although attractive in its simplicity and ease of measurement, this expression only considers the direct contribution of mutual coupling to the antenna correlation, the properties of the incident RF field and its interaction with the antennas' gain patterns are not considered in this expression.

3. PIFA-MIMO Antenna System

Due to the low profile and easy to match of the PIFA antennas, Mobile phone built-in antenna always adopts PIFA (Planar inverted F antenna) antennas. This part presents a design of 4×4 MIMO antenna system model, operating in 2.4 GHZ (ISM band). The antenna system uses air as the medium. Because of the four antenna elements sharing one floor, the current of one antenna element will be coupled to another antenna element through the floor, which leads to mutual coupling and reduces the isolation between antenna elements. The antenna system adopts defect ground structure to extending the current length, as a result, effectively reducing the mutual coupling between the antenna elements. In addition, the antenna space-coupling by space radiation field will influence the performance of the MIMO antenna system. In this chapter, the four port antenna elements of this antenna system are placed vertically with each other, reducing the space-coupling between antenna units, increasing the isolation. Simulation results show that the antenna can meet the performance requirements of the MIMO antenna systems.

3.1. Antenna Structure

Figure 1 shows a planar and solid structure. The antenna system is composed of four parts, the radiation patch, the feed structure, the short circuit unit and the floor. In the design, the medium filled with air is between antenna radiation patch and the floor. Four identical PIFA antennas are located at the four corners of the floor. The
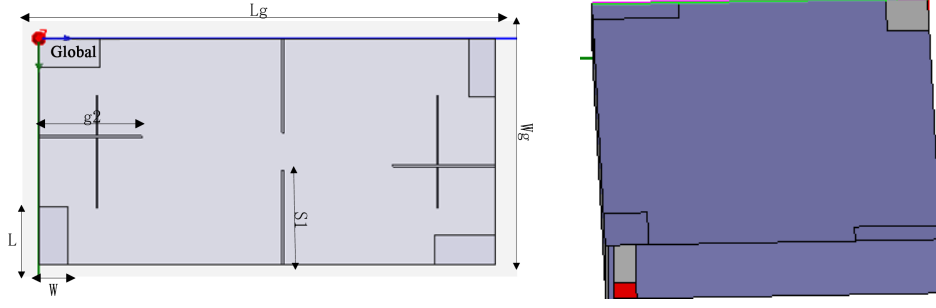
Figure 1. Antenna structure.

overall size of the machine is $120 \times 60 \times 10$ mm^3, and the size of each PIFA antenna element is $16 \times 7.5 \times 10$ mm^3.

The specific size of antenna elements: Lg = 120 mm, Wg = 60 mm, L = 16 mm, W = 7.5 mm, S1 = 27 mm, g2 = 30 mm.

As shown in **Figure 1**, two "十" shaped slots and two line-shaped slots are etched on the ground, as well as, four antenna units are arranged vertically between each other to reduce the space-coupling.

3.2. Antenna Simulation Results

Using the simulation software (HFSS) to simulate the antenna model, as shown in **Figure 2(a)**, the operating frequency of the four PIFA antennas (−15 dB) all cover 2360 - 2420 MHZ, meeting the performance requirements of the mobile phone MIMO antenna in 3G and 4G-LTE band; **Figure 2(b)** is the mutual correlation coefficient between two antennas, the correlation coefficient of the antenna system in operating band is basically below −15 dB. Using the simulation software (HFSS), the antenna radiation pattern data can be obtained, and then importing the data into the software of Matlab, according to the Equation (9) shown above, envelope correlation coefficient curve between adjacent antenna elements is shown in **Figure 3**. In the calculation, we always assume that the incident field in horizontal and vertical direction was uniformly distributed, XPR is 6 dB. The ρ_e in center frequency is that, $\rho_e = 0.0054$. Hence, the isolation between antennas elements meets well the requirements of mobile antenna systems for isolation.

4. Monopole-MIMO Antenna with Large Bandwidth

4.1. Antenna Structure

Printed monopole antenna has been widely used in many wireless devices due to its low cost, light weight and easy processing. As a new type of antenna, high dielectric antenna has the advantages of small size, simple structure and low cost. With the application of 4G wireless communication, the MIMO antenna systems operating in 3G and 4G-LTE frequency band have a good application prospect and demand. In order to achieve the large bandwidth of the antenna system, this paper mainly uses the multi-branch technology to achieve the principle of multi-resonant, through connecting the two or more adjacent resonant frequency band together, hence, obtaining the expansion of the bandwidth.

In this paper, the design of a broadband monopole-MIMO antenna system is composed of four monopole printed antennas, floor and dielectric substrate. The overall structure of the antenna system is shown in **Figure 4**. Four monopole antennas are printed on the four sides of the FR4 substrate, and the floor is located at the bottom of the substrate. In order to achieve the large bandwidth of the antenna, the multi branch structure is adopted to realize the multi resonance. The sizes of the antenna system are shown as: p1 = 21.25 mm, p2 = 9.5 mm, p3 = 38 mm, p5 = 21.5 mm, Lg = 60 mm, Wg = 46 mm.

4.2. Antenna Simulation Results

By simulation, the return loss of the four single pole printed antennas is shown in **Figure 5**. The operating frequency of the four antenna elements (S11 < −6 dB) covers the 3G and 4GLTE bands, and the large bandwidth of the MIMO antenna system is realized.

(a)

(b)

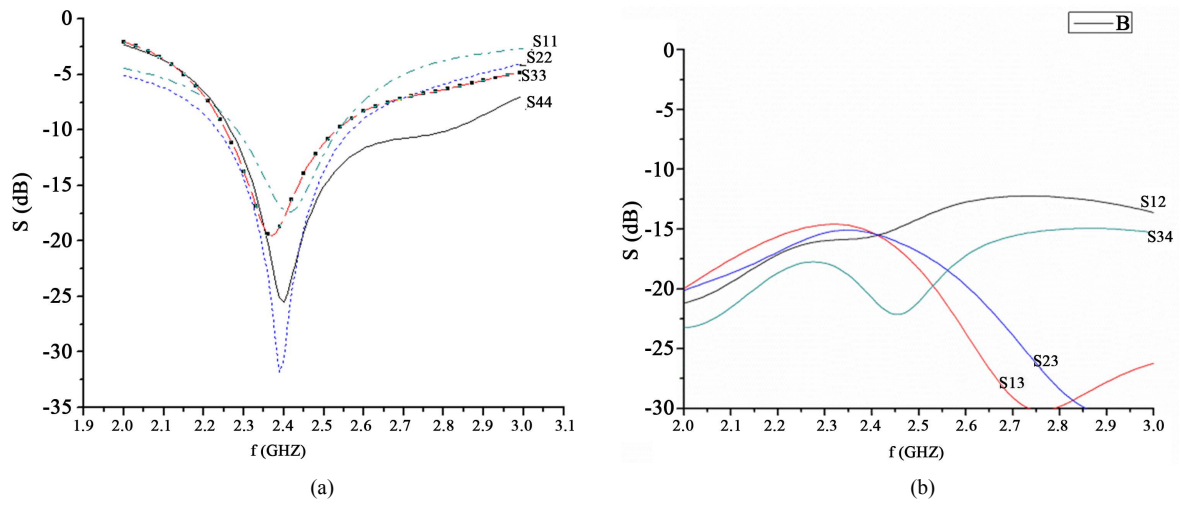**Figure 2.** (a) The curves of S22, S33, S11 and S44; (b) The curves of S12, S13, S23 and S34.
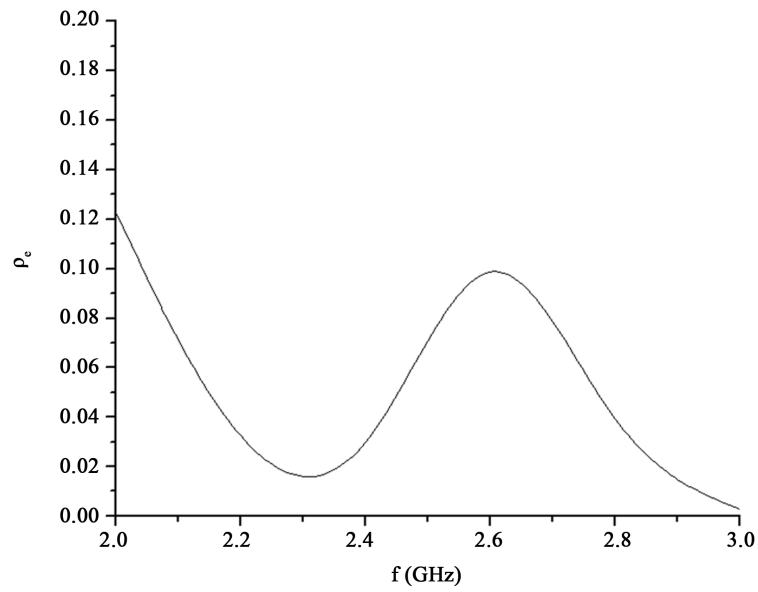

Figure 3. The curve of ρ_e.
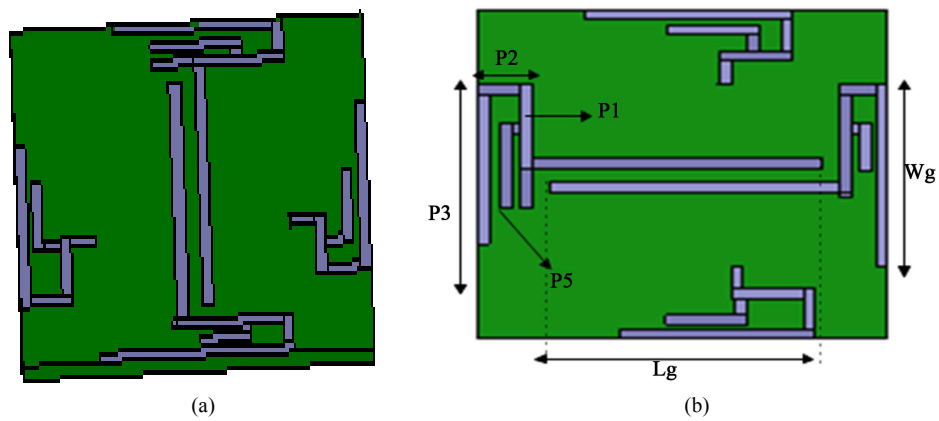

(a)

(b)

Figure 4. Top structure of antenna.

The MIMO antenna system designed in this paper is composed of four printed monopole antennas with nearly identical multi branch. The four antenna elements are located on the four side of the dielectric substrate respectively, without floor under the antenna elements. In order to obtain a better impedance matching and increase the isolation between adjacent antenna units, the floor under the medium substrate is slotted; the slotted size is 46 mm × 1 mm, so that the floor is divided into two parts, as shown in **Figure 6**. Using Equation (9), the ρ_e between the antenna units can reach the magnitude of 0.01, far less than 1. According the result above, the antenna system can work well in operating frequency band.
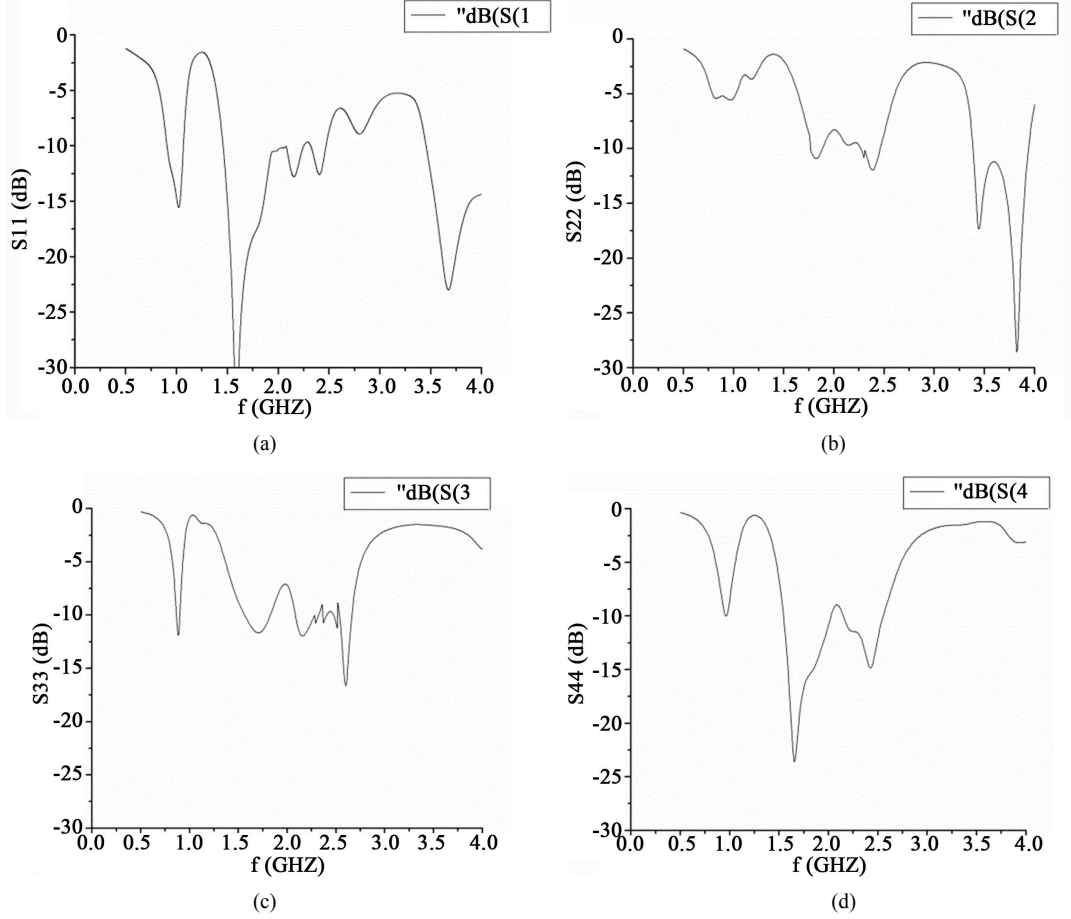

(a) (b) (c) (d)
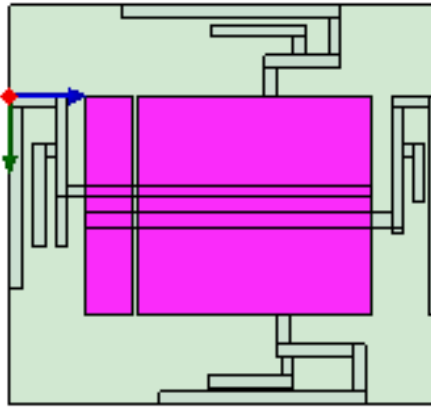
Figure 5. Antenna return loss.

Figure 6. Antenna structure.

5. Conclusion

In this paper, Section 1 mainly introduces the present status of research on MIMO antenna systems at home and abroad. In Section 2, an algorithm calculating envelope correlation coefficient between MIMO antenna elements is proposed. The third chapter and the fourth chapter designed a PIFA-MIMO antennas system and a monopole MIMO antennas system respectively, which were all widely used in the design of antennas system in mobile phone. And based on the formula calculating ρ_e (envelope correlation coefficient) in Section 2, the ρ_e between antenna elements were also calculated in Section 3 and Section 4. The calculation results show that the two antennas systems can meet the performance requirements well.

References

[1] Sun, X.Y. and Xu, P.F. (2015) Analysis of Channel Capacity of Wireless MIMO Systems. *Computer and Telecom*, **7**, 35-38.

[2] Lee, W.-W. and Rhee, B.-H. (2013) Characterization of Performance of a Mobile MIMO Antenna in Free Space. *IEEE Antennas and Wireless Propagation Letters*, **12**, 1153-1156. http://dx.doi.org/10.1109/LAWP.2013.2280465

[3] Tang, T.-C. and Lin, K.-H. (2014) An Ultra-Wideband MIMO Antenna with Dual Band-Notched Function. *IEEE Antennas and Wireless Propagation Letters*, **13**, 1076-1079. http://dx.doi.org/10.1109/LAWP.2014.2329496

[4] Shoaib, S., Shoaib, I., Shoaib, N., Chen, X.D. and Parini, C.G. (2014) Design and Performance Study of a Dual-Element Multiband Printed Monopole Antenna Array for MIMO Terminals. *IEEE Antennas and Wireless Propagation Letters*, **13**, 329-332. http://dx.doi.org/10.1109/LAWP.2014.2305798

[5] Wang, F.Y., Liang, R.X., Gong, S.X., *et al*. (2013) Defected Ground Structure Applied to the Dual-Band MIMO Antennas Systems. *Microwave Journal*, **1**, 25-29.

[6] Prasanna, K.M. and Behera, S.K. (2013) Compact Two-Port UWB MIMO Antenna System with High Isolation Using a Fork-Shaped Structure. *IEEE* 2013 *International Conference on Communications and Signal Processing* (*ICCSP*), Melmaruvathur, 3-5 April 2013, 726-729. http://dx.doi.org/10.1109/iccsp.2013.6577151

[7] Ren, J., Hu, W., Yin, Y.Z. and Fan, R. (2014) Compact Printed MIMO Antenna for UWB Applications. *IEEE Antennas and Wireless Propagation Letters*, **13**, 1517-1520. http://dx.doi.org/10.1109/LAWP.2014.2343454

[8] Kiem, N.K., Phuong, H.N.B., Hieu, Q.N. and Chien, D.N. (2013) A Compact Printed 4×4 MIMO-UWB Antenna with WLAN Band Rejection. 2013 *IEEE Antennas and Propagation Society International Symposium* (*APSURSI*), Orlando, 7-13 July 2013, 2245-2246. http://dx.doi.org/10.1109/APS.2013.6711781

[9] Khan, M.S., Capobianco, A.D., Asif, S., Iftikhar, A., Ijaz, B. and Braaten, B.D. (2015) Compact 4×4 UWB-MIMO Antenna with WLAN Band Rejected Operation. *Electronics Letters*, **51**, 1048-1050. http://dx.doi.org/10.1049/el.2015.1252

[10] Li, L. (2012) Research on Correlation Matrix and Correlation Coefficient of Receiving Signal in Antenna. http://www.docin.com/p-347946681.html